International Tables for Crystallography (2006). Vol. B, Figure 4.2.3.6, p. 416.

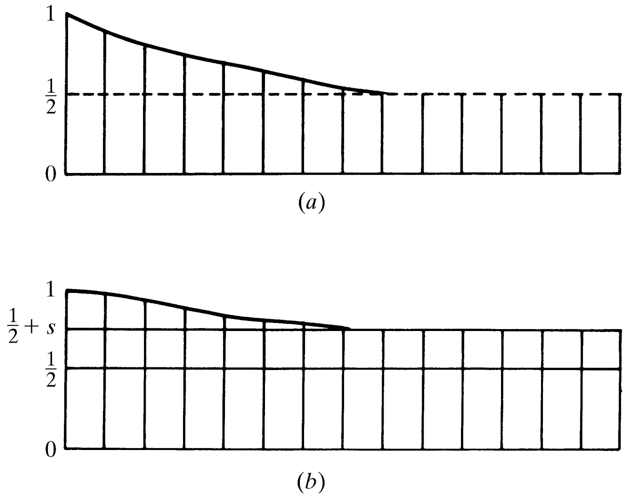

Fig. 4.2.3.5. Typical distributions of mixed crystals (unmixing): (*a*) upper curve: short-range order only; (*b*) lower curve: long-range order.

interpretation of the diffraction pictures this correlation may be derived from the diffraction pattern itself. The $p_{\mu\mu'}(\mathbf{m})$ are separable into a strictly periodic and a monotonically decreasing term approaching zero in both cases. This behaviour is shown in Figs. 4.2.3.6(*a*), (*b*). The periodic term contributes to sharp Bragg scattering. In the case of short-range order the symmetry relations given in equation (4.2.3.25) are valid. The convolution in real space yields with factors $t(\mathbf{r})$ (equations 4.2.3.21):

$$\begin{aligned}&\tfrac{1}{2}t(\mathbf{r})[\textstyle\sum_{\mathbf{m}}\delta(\mathbf{r}+\mathbf{m})p'_{11}(\mathbf{m})]*F_1(\mathbf{r})*F_1(-\mathbf{r})\\&+\tfrac{1}{2}t(\mathbf{r})[\textstyle\sum_{\mathbf{m}}\delta(\mathbf{r}+\mathbf{m})p'_{12}(\mathbf{m})]*F_1(\mathbf{r})*F_2(-\mathbf{r})\\&+\tfrac{1}{2}t(\mathbf{r})[\textstyle\sum_{\mathbf{m}}\delta(\mathbf{r}+\mathbf{m})p'_{21}(\mathbf{m})]*F_2(\mathbf{r})*F_1(-\mathbf{r})\\&+\tfrac{1}{2}t(\mathbf{r})[\textstyle\sum_{\mathbf{m}}\delta(\mathbf{r}+\mathbf{m})p'_{22}(\mathbf{m})]*F_2(\mathbf{r})*F_2(-\mathbf{r}),\end{aligned}$$

where $p'_{\mu\mu'}(\mathbf{m})$ are factors attached to the δ functions:

$$\begin{aligned}p'_{11}(\mathbf{m})&=p_{11}(\mathbf{m})-\tfrac{1}{2}=p'_{22}(\mathbf{m})\\p'_{12}(\mathbf{m})&=p'_{21}(\mathbf{m})=-p'_{11}(\mathbf{m}).\end{aligned}$$

The positive sign of n in the δ functions results from the convolution with the inverted lattice [*cf.* Patterson (1959, equation 32)]. Fourier transformation of the four terms given above yields the four corresponding expressions (μ, μ'!):

$$\tfrac{1}{2}[T(\mathbf{H})*\textstyle\sum_{\mathbf{m}}p'_{\mu\mu'}(\mathbf{m})\exp\{-2\pi i\mathbf{H}\cdot\mathbf{m}\}]F_\mu(\mathbf{H})F^+_{\mu'}(\mathbf{H}). \quad (4.2.3.27a)$$

Now the summation over $\mathbf{m}$ may be replaced by an integral if the factor $l(\mathbf{m})$ is added to $p'_{\mu\mu'}(\mathbf{m})$, which may then be considered as the smoothest continuous curve passing through the relevant integer values of $\mathbf{m}$:

$$\textstyle\sum \rightarrow \int l(\mathbf{m})p'_{\mu\mu'}(\mathbf{m})\exp\{-2\pi i\mathbf{H}\cdot\mathbf{m}\}\,\mathrm{d}\mathbf{m}$$

since both $l(\mathbf{m})$ and $p'_{\mu\mu'}(\mathbf{m})$ are symmetric in our special case we obtain

$$\textstyle\sum = L(\mathbf{H})*P'_{\mu\mu'}(\mathbf{H}).$$

Insertion of the sum in equation (4.2.3.27*a*) results in

$$\tfrac{1}{2}[L(\mathbf{H})*T(\mathbf{H})*P'_{\mu\mu'}(\mathbf{H})]F_\mu(\mathbf{H})F^+_{\mu'}(\mathbf{H}). \quad (4.2.3.27b)$$

Using all symmetry relations for $p'_{\mu\mu'}(\mathbf{m})$ and $P'_{\mu\mu'}(\mathbf{H})$, respectively, we obtain for the diffuse scattering after summing over μ, μ'

$$I_d \approx [L(\mathbf{H})*T(\mathbf{H})*P'_{11}(\mathbf{H})]|\Delta F(\mathbf{H})|^2 \quad (4.2.3.28)$$

with $\Delta F(\mathbf{H}) = \frac{1}{2}[F_1(\mathbf{H}) - F_2(\mathbf{H})]$.

It should be borne in mind that $P'_{11}(\mathbf{H})$ decreases rapidly if $p'_{11}(\mathbf{r})$ decreases slowly and *vice versa*. It is interesting to compare the different results from equations (4.2.3.21*b*) and (4.2.3.28). Equation (4.2.3.28) indicates diffuse maxima at the positions of the sharp Bragg peaks, while the multiplication by $D(\mathbf{H})$ causes satellite reflections in the neighbourhood of Bragg maxima. Both equations contain the factor $|\Delta F(\mathbf{H})|^2$ indicating the same influence of the two structures. More complicated formulae may be derived for several cell occupations. In principle, a result similar to equation (4.2.3.28) will be obtained, but more interdependent correlation functions $p_{\mu\mu'}(\mathbf{r})$ have to be introduced. Consequently, the behaviour of diffuse intensities becomes more differentiated in so far as all $p'_{\mu\mu'}(\mathbf{r})$ are now correlated with the corresponding $\Delta F_\mu(\mathbf{r}), \Delta F_{\mu'}(-\mathbf{r})$. Hence the method of correlation functions becomes increasingly ineffective with increasing number of correlation functions. Here the cluster method seems to be more convenient and is discussed below.

(6) *Lamellar domains with long-range order: tendency to exsolution*

The Patterson function of a disordered crystal exhibiting long-range order is shown in Fig. 4.2.3.5(*b*). Now $p_{11}(\infty)$ converges against $\frac{1}{2}+s$, the *a priori* probability changes correspondingly. Since $p_{12}(\infty)$ becomes $\frac{1}{2}-s$, the symmetry relation given in equation (4.2.3.25) is violated: $p_{11}(\mathbf{r}) \neq p_{22}(\mathbf{r})$ for a finite crystal; it is evident that another crystal shows long-range order with the inverted correlation function, $p_{22}(\underline{\infty}) = \frac{1}{2}+s$, $p_{21}(\underline{\infty}) = \frac{1}{2}-s$, respectively, such that the symmetry $p_{11}(\mathbf{r}) = p_{22}(\mathbf{r})$ is now valid for an assembly of finite crystals only. According to Fig. 4.2.3.5(*b*) there is a change in the intensities of the Bragg peaks.

$$\begin{aligned}I_1 &\sim |(\tfrac{1}{2}+s)F_1(\mathbf{H})+(\tfrac{1}{2}-s)F_2(\mathbf{H})|^2\\I_2 &\sim |(\tfrac{1}{2}+s)F_2(\mathbf{H})+(\tfrac{1}{2}-s)F_1(\mathbf{H})|^2,\end{aligned} \quad (4.2.3.29)$$

where I_1, I_2 represent the two solutions discussed for the assembly of crystals which have to be added with the probability $\frac{1}{2}$; the intensities of sharp reflections become

$$I = (I_1 + I_2)/2. \quad (4.2.3.30)$$

Introducing equation (4.2.3.29) into (4.2.3.30) we obtain

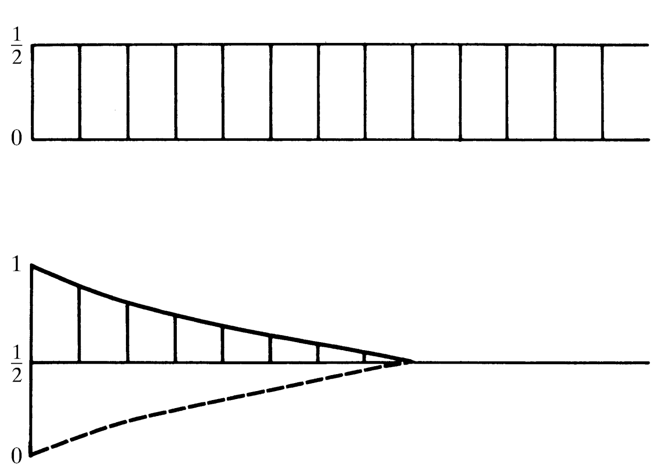

Fig. 4.2.3.6. Decomposition of Fig. 4.2.3.5(*a*) into a periodic and a rapidly convergent part.

references